IJPE_Effect of input_Q1_2019

by Sri Atmaja Rosyidi
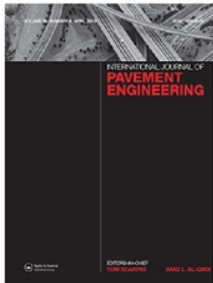
Effect of input source energy and measurement of flexible pavement deflection using the SASW method

Norfarah Nadia Ismail, Nur Izzi Md. Yusoff, Khairul Anuar Mohd Nayan, Norinah Abd Rahman, Sri Atmaja P. Rosyidi & Amiruddin Ismail

Taylor & Francis
Taylor & Francis Group

Effect of input source energy and measurement of flexible pavement deflection using the SASW method

Norfarah Nadia Ismail[a], Nur Izzi Md. Yusoff[a], Khairul Anuar Mohd Nayan[a], Norinah Abd Rahman[a], Sri Atmaja P. Rosyidi[b] and Amiruddin Ismail[a] [ID]

[a]Department of Civil and Structural Engineering, Universiti Kebangsaan Malaysia, Selangor, Malaysia; [b]Department of Civil and Structural Engineering, Universitas Muhammadiyah Yogyakarta, Yogyakarta, Indonesia

ABSTRACT

This paper presents the effect of input source energy on the results of spectral analysis of surface wave (SASW) evaluation of flexible pavements in terms of maximum and minimum wavelength. A series of surface wave tests, namely the SASW test, were done on asphalt pavement using four steel balls with different masses as sources. These sources were dropped from two different heights, 0.25 and 0.50 m. This test was also conducted with two different configurations, i.e. with the receivers positioned 0.15 and 0.30 m apart. This paper also presents the feasibility of using accelerometers to measure flexible pavement deflection. For this purpose, the process of integrating accelerometer time history is described. It is proved that a change in input source energy has some effect on the value of maximum and minimum wavelength. The result for numerical double integration is satisfactory and is congruent with the displacement obtained through finite element analysis.

1. Introduction

The use of surface wave in seismic testing has gained popularity in engineering practice as a method for determining shear wave velocity profile (Stokoe *et al.* 2004, Lin and Lin 2007). The surface wave testing in engineering, which have been used quite extensively for quite some time, is associated with the two-station set-up used in the spectral analysis of surface wave (SASW) method (Kausel and Roesset 1981, Nazarian *et al.* 1988, Rix and Stokoe 1989, Gucunski and Woods 1991, Nazarian and Desai 1993). The systematic introduction of the seismic surface wave method to engineering applications has resulted in an increased use of this non-destructive testing technology (Nazarian and Stokoe 1986). In general, SASW has been widely used as a non-destructive test for evaluating subsurface parameters in soils and pavements. SASW utilises Rayleigh waves which propagate at different velocities depending on frequency. The dispersive characteristics of Rayleigh waves propagating through a layered material were measured and were then used to delineate the modulus profile of a pavement section and also to evaluate the S-wave profile of the material (Stokoe *et al.* 1994, Stokoe *et al.* 2004). Dispersion curve is a plot of variation in Rayleigh wave phase velocity against wavelength or frequency (Kumar and Naskar 2015).

The SASW method is a simple technique which could be easily implemented in the field. It has a source–receiver configuration with multiple sources which are carefully selected for the measured wavelength range of each source–receiver configuration,

and therefore provide high-quality results. Phase velocities are calculated from the phase difference. The key feature of SASW method is that it measures apparent velocities, which correspond to the superposed mode of higher mode surface waves and body waves. Determination of apparent phase velocities incorporates phase unwrapping. The phase unwrapping procedure often requires experienced personnel making the best decision during the unwrapping process. However, the non-systematic nature of unwrapping a phase could be improved with a signal processing technique, such as the impulse response filtration technique (Joh *et al.* 1997) and Gabor spectrum.

SASW is capable of accurately defining the elastic moduli and the thickness of layered systems, such as soil and pavement, with a particular advantage of it being performed entirely on the surface (Gucunski and Woods 1992). In general, waves travel at high velocity (and high frequency) in pavement materials. It is known that the higher frequency waves are associated with shorter wavelength and, as a result, these waves propagate only at shallow depths. On the other hand, lower frequency waves have longer wavelength and travel through deeper layers (Jones 1962, Heisey *et al.* 1982, Nazarian 1984). For asphalt pavements, the ground is excited using a small impact source to generate waves propagating at shallow depth. Roesset *et al.* (2011) stated that: (1) an increase in the height of the dropping mass led to an increase in impact velocity and contact force; and (2) an increase in the dropping mass results in an amplification of the low frequency components of the Fourier Spectrum of the contact force (Kumar and Naskar 2015).

CONTACT Norfarah Nadia Ismail ✉ norfarahnadia@gmail.com

Very recently, several studies were conducted to evaluate pavements using the SASW method through the use of a spherical mass dropped from different heights (Kumar 2011, Kumar and Rakaraddi 2012, Kumar and Rakaraddi 2013a, 2013b, Kumar and Hazra 2014a, 2014b, Kumar and Naskar 2015). A study on concrete pavements conducted by Kumar and Hazra in 2014 found that the value of maximum and minimum wavelength is a function of the magnitude of the input source energy. The researchers also confirmed the usefulness of SASW technique in exploring the shear wave velocity profiles of different pavement layers. In 2012, Kumar and Rakaraddi revealed that there is a need to consider the height of fall of dropping weight in SASW testing. Their 2013 research showed that the distance between the source and first receiver for cement concrete pavements should be greater than the distance for asphaltic pavements. Their finding showed that the acceptable distance for tests on asphaltic pavements is 0.5–0.75 m. This paper improves the findings of these studies, in that this study was applied to the condition of asphaltic pavement in Malaysia, with the recommendation and addition of variation in receiver distance.

This study was also conducted to investigate the feasibility of using accelerometers to measure road deflection. Measurement of road deflection due to traffic loading always requires complex installation of sensors and is often regarded as a trivial job. This paper proposed the use of accelerometers as a small yet reliable sensor to measure road deflection by performing numerical double integration. Currently, other than geophones, accelerometers are one of the devices widely used to obtain either dynamic measurements, which are mainly used to measure track deflection (Hall 2003, Bowness et al. 2007, Priest and Powrie 2009, Jiang, Bian, Cheng, et al. 2016, Jiang, Bian, Jiang, et al. 2016, Sayeed and Shaheen 2016), or static measurement, such as bridge deflection (Roberts et al. 2001) and road deflection (Arraigada and Partl 2006, Simonin et al. 2009). The installation of the sensors is practical and easy, with the robust POLLCA hardware providing a lot of advantage due to its handling mobility and portability. The use of POLLCA could be a low-cost solution for the measurement of road deflection in industry.

From this measurement, the recorded time series were used to measure deflection. This paper shows the feasibility of using the measurement obtained from using accelerometers to measure road deflection. According to Simonin et al. (2009), road deflection measurement is the first element in evaluating road bearing capacity. The measurement level, however, quickly changes along the roadway. Thus, the placement of the measurement device (in this case, accelerometer) on road surface is crucial to ensure accurate results.

2. Methodology

A series of field tests were carried out to investigate the effect of input energy on SASW evaluation in terms of maximum and minimum wavelength. The SASW method makes use of the determination of phase difference between two receivers over a wide range of frequencies. With regard to data collection for the experiment, the equipment and testing configuration used in this test is closely related to the scope of the test and the technique to be used in the interpretation of the results. In order to determine the length of the measurement, the desired depth of investigation must always be taken into account. The relationship between frequency, wavelength and phase velocity makes the frequency range of interest closely related to the materials to be investigated. For example, deep penetration in soft soils requires lower frequency components (Roesset 1998). Therefore, preliminary information, or á-priori' knowledge, regarding the site being investigated is very helpful.

2.1. Testing equipment

The basic equipment used in the SASW test comprised of receivers (accelerometers) connected to an acquisition device which digitises and stores seismic signals. The desired depth of penetration will determine the appropriate type of receivers and the specifications required. Various types of recording equipments, the main function of which is to digitise and record analog electric signals generated by the receivers, could be used. The use of digital signal analyzer allows signal to be processed in real-time, therefore quality assessment and preliminary interpretation could be performed instantly on site. In this test, data were recorded using a Portable Outdoor Laptop with a Customized Compact Analyzer (POLCCA). It is a portable field laptop with built-in dynamic signal analyzer. In this test, which was done on asphalt pavement, steel balls 25.4, 38.1, 50.8 and 76.2 mm in diameters were used.

2.1.1. Sources in SASW Testing

Several sources were used in the SASW testing to excite the ground, induce vibration and produce waves which travel through the layered systems (in this case the asphaltic pavement). Different types of sources can be used, which range from ordinary hammers to expensive controlled source. Controlled sources allow for the collection of high-quality data with high signal to noise ratio.

Sources are typically applied by dropping weights of different sizes (Roesset 1998). For further source offset which requires longer frequency range to penetrate deeper into the ground, an ordinary impact hammer might not be sufficient. Therefore, heavier sources are required. In this test, the sources used were four steel balls with varying mass and diameter, as shown in Figure 1.
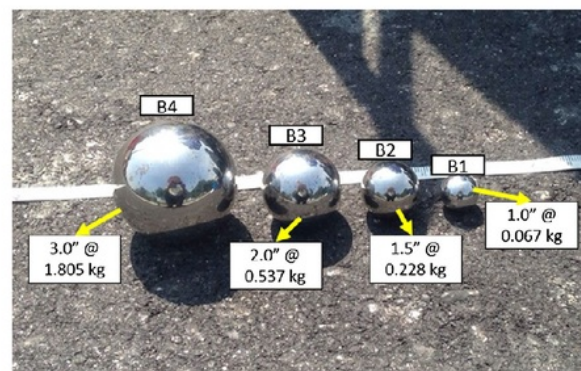

Figure 1. Steel balls with different diameters and masses, m used in the test.

Table 1. Characteristics of the accelerometer according to manufacturer's specification.

Series	C68
Sensitivity (±10%)	100 mV/g
Measurement range	50 g pk
Frequency range (±10%)	0.3–12,000 Hz
Resonant frequency	≥35 kHz
Spectral noise (10 Hz)	16 µg/√Hz

2.1.2. Sensors

In order to choose an appropriate sensor with the desired specification, it is necessary to relate it with the desired depth of penetration. The typical frequency range for pavements is between 1000 and 15,000 Hz, and this makes accelerometers the best sensors for measurement on pavements as it has higher resonance frequency compared to geophones.

For pavement testing where the frequency range is of particular interest, or when testing stiffer materials where the desired depth is shallow, accelerometers are typically used as receivers. Accelerometers can reach operative frequencies in the kHz range and as with any other types of dynamic sensors, data can be synthesised in the time or frequency domain. Accelerometers are for the most part micro-electromechanical systems, or MEMS. The basic principle operating behind the MEMS accelerometer is the displacement of a small proof mass marked onto the silicon surface of the integrated circuit (IC) and suspended by small beams. As acceleration is applied to the device, a force develops which displaces the mass. Support beams act as a spring, and fluid (usually air) trapped inside the IC acts as a damper, resulting in a second-order lumped physical system.

In this study, accelerometers are used to acquire time history data to detect small vibration signals with good accuracy. It is chosen based on factors such as frequency response, sensitivity and noise tolerance. The details of the sensor are presented in Table 1.

2.2. Test configuration

For the field test, two accelerometers were located in an array for two types of configurations. In the first configuration, the accelerometers were positioned 0.15 m apart, and in the second configuration, the accelerometers were positioned 0.30 m apart. Both accelerometers were mounted with weights, as shown in Figure 2, to ensure good coupling between accelerometers and pavement surface. For the first configuration, three source distances, 0.15, 0.3 and 0.6 m, from the first receiver were used. For the second configuration, the sources were positioned 0.30, 0.6 and 1.2 m from the first receiver. Steel balls were used as a source and measurements were recorded for both configurations and for all source distances. The tests were carried out by dropping the steel balls from two different heights, 0.25 and 0.50 m. Figure 3 shows the distance layout of the receiver, the distance of the sources and height of the dropping balls. Input source energy is plotted in Joule, and is calculated using Equation (1):

$$ \text{Energy} = mgh \tag{1} $$

where m is mass of the dropping ball (kg), g is the acceleration due to gravity (9.81 ms^{-2}) and h is height of fall of the ball (m).
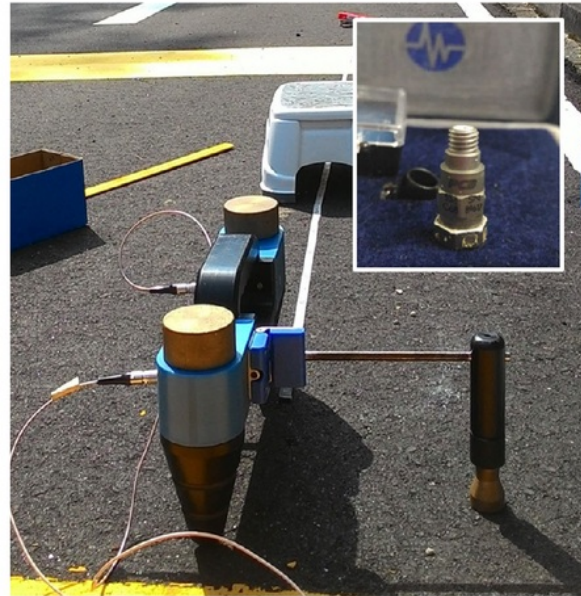

Figure 2. Weight-mounted accelerometers used during measurement.

2.3. Numerical integration of acceleration

It is generally known that acceleration time history can be used to obtain displacement. This can be done by applying double integration to the acceleration data signal. Although theoretically it looks like a straightforward procedure, it is actually much trickier than it actually seems. The acceleration data signal must be firstly numerically integrated to obtain velocity, and thereafter numerically integrated again (this is the second integration) to obtain displacement. Numerical double integration of acceleration data signal involves errors that should be carefully studied and minimised. Errors could occur because, when integrating, low frequency contents of the waveform are greatly amplified, high frequencies are reduced and hence the phase is changed (Arraigada and Partl 2006). These problems, if not studied and handled properly, could affect and dominate the final result of the calculated displacement. In this paper, however, there is no frequency domain and hence no phase change. Also, a bandpass filter was applied during calculation to control the cut-off frequency accurately.

The displacement, velocity and acceleration parameters are closely related to one another (Arraigada and Partl 2006). Conversion can be done using the digital signal processing procedure by performing a single or double integration. Mathematically, displacement can be calculated from acceleration using Equation (2):

$$ d_c(t) = d_0 + v_0 t + \int_0^t \mathrm{d}t \int_0^\tau a(\tau)\mathrm{d}\tau \tag{2} $$

where d_0 is initial displacement at $t = 0$, v_0 is initial velocity at $t = 0$ and d_c is calculated displacement at t.

It is known that the above equation is applied only for continuous (analog) function. Equation (3) can be used for a numerical
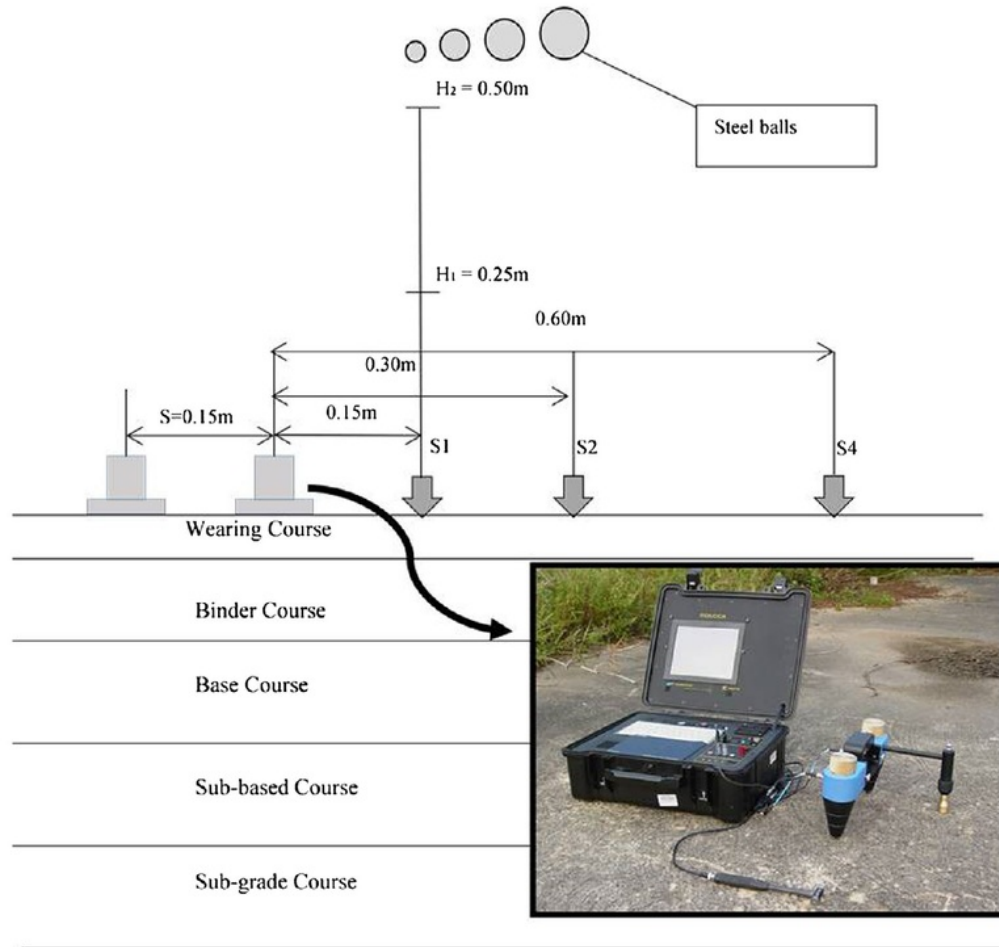
Figure 3. Layout of the SASW test configuration, with POLCCA.

integration (applied when the signal is discrete or digital) in the time domain:

$$\int_{t(0)}^{t(n)} a(t)dt \cong \sum_{I=1}^{n} \left(\frac{a(1-i) + a(i)}{2} \right) \Delta t \qquad (3)$$

where $a(t)$ is continuous time domain waveform, $a(i)$ a is ith sample of the time waveform, Δt is time increment between sample $(t(i) - t(i-1))$ and n is number of sample of the digital record.

Velocity then can be computed from the acceleration signal using Equation (4), and thereafter displacement can be calculated using Equation (5):

$$v_c(i) = v_c(i-1) + \frac{a(1-i) + a(i)}{2} \Delta t \qquad (4)$$

and

$$d_c(i) = d_c(i-1) + \frac{v(1-i) + v(i)}{2} \Delta t \qquad (5)$$

where $a(i)$ is ith sample of acceleration waveform, $v_c(i)$ is ith sample of calculated velocity and $d_c(i)$ is ith sample of calculated displacement.

In his paper, Joh (Joh *et al.* 2014) elaborated on velocity integration and its verification through laboratory tests such as LVDT measurements and potentiometer measurements. Numerical double integration is also discussed by Arragaida (Arraigada and Partl 2006) with verification of lab result from LVDT monitoring.

3. Results and discussion

3.1. Effect of input source energy

In order to obtain a reliable evaluation of stiffness profile, a single source and receiver set-up is not sufficient to determine the phase velocity over a wide range of wavelengths. Therefore, several measurement set-ups incorporating several source locations should be used. This source offset concept was used during field measurement. For a receiver distance of 0.15 m, the source offset is kept constant at 0.15, 0.30 and 0.60 m from the first receiver. The dispersion curve is a combination of three individual dispersion curves from three locations of source offset. Figure 4 shows the dispersion curves obtained using all four balls as sources with 0.15 m receiver distance, at dropping heights 0.25 and 0.50 m, respectively.
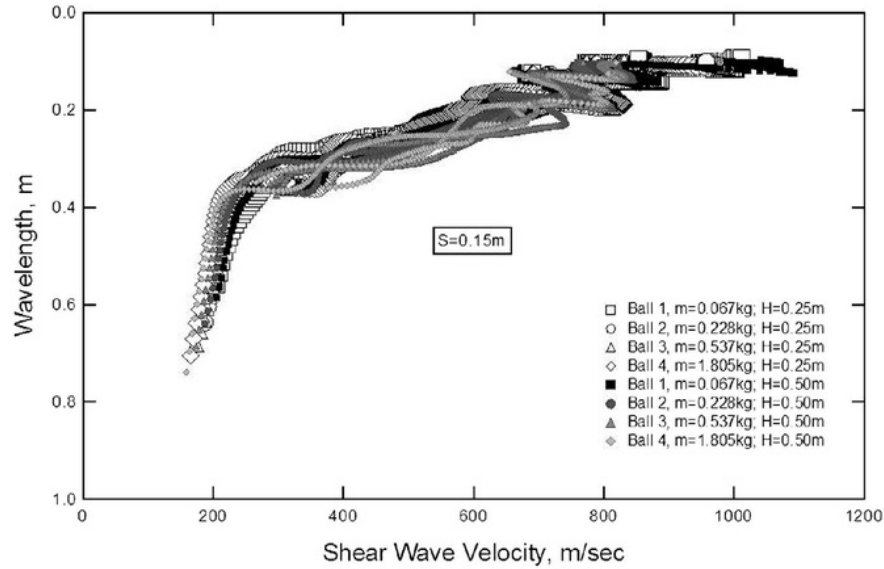
Figure 4. Dispersion curves from SASW measurements with 0.15 m receiver distance for height of dropping mass 0.25 and 0.50 m.

Figure legend:
- □ Ball 1, m=0.067kg; H=0.25m
- ○ Ball 2, m=0.228kg; H=0.25m
- △ Ball 3, m=0.537kg; H=0.25m
- ◇ Ball 4, m=1.805kg; H=0.25m
- ■ Ball 1, m=0.067kg; H=0.50m
- ● Ball 2, m=0.228kg; H=0.50m
- ▲ Ball 3, m=0.537kg; H=0.50m
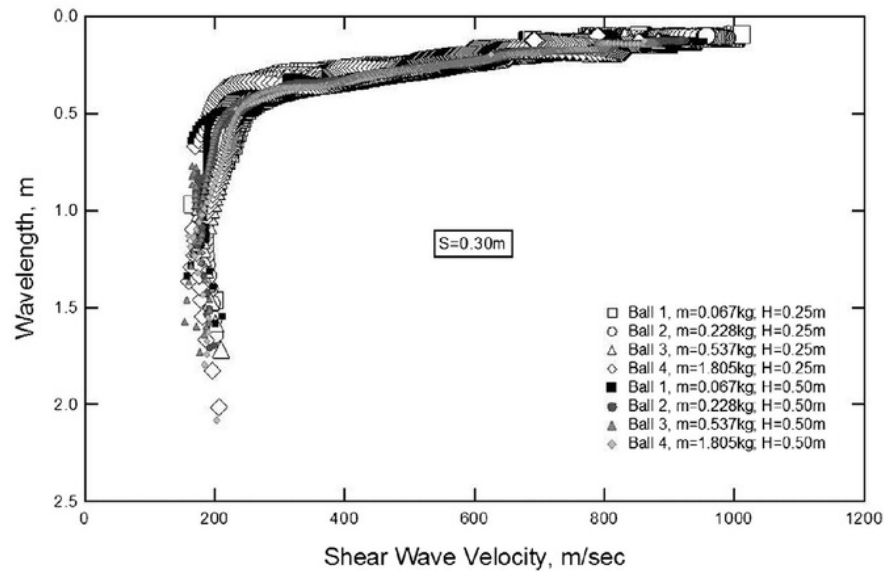- ◆ Ball 4, m=1.805kg; H=0.50m

Figure 5. Dispersion curves from SASW measurements with 0.30 m receiver distance for height of dropping mass 0.25 and 0.50 m.

For a receiver distance of 0.30 m, the source offset is kept constant at 0.30, 0.60 and 1.2 m from the first receiver. Figure 5 shows the dispersion curves obtained using all four balls as sources with 0.30 m receiver distance, at both 0.25 and 0.50 m dropping heights. Both measurement set-ups are shown in Figures 4 and 5; the figures show that the increase in steel balls with larger mass or diameter yielded higher values of λ_{min} and λ_{max}.

It can also be proven that for both heights of dropping ball, the ball with the largest mass, namely Ball 4, produced the largest wavelength, and vice versa. Ball 4 not only has the highest mass but also the largest diameter, which means larger surface contact between the pavement surface and the steel ball. It therefore resulted in a longer duration of contact time. Previous studies have shown that the duration of impact has a profound effect on the dominant spectral content of the emerging signal (Kumar and Hazra 2014a, 2014b, Barness and Trottier 2009a, Barness and Trottier 2009b). This has been distinguished in this research, as evident in both Figures 4 and 5, which shows that impacts of long duration generate low frequency signals which in turn result in deeper exploration depth. On the other hand, smaller balls generate high frequency signals which produced shorter duration impacts.

For the different heights of fall of the dropping mass, the values for λ_{min} and λ_{max} were obtained from the dispersion plots and these values are tabulated in Table 2 for a receiver distance of

Table 2. Comparison of λ_{min} and λ_{max} values for different drop heights of steel balls for a receiver distance of 0.15 m.

Ball no	Ball diameter (mm)	Height of fall, H (m)			
		0.25		0.50	
		λ_{max} (m)	λ_{min} (m)	λ_{max} (m)	λ_{min} (m)
1	25.40	0.5585	0.0939	0.5864	0.0979
2	38.10	0.6371	0.1012	0.6389	0.1013
3	50.80	0.6809	0.1025	0.6856	0.1028
4	76.20	0.7057	0.1029	0.7392	0.1032

Table 3. Comparison of λ_{min} and λ_{max} values for different drop heights of steel balls for a receiver distance of 0.30 m.

Ball no	Ball diameter (mm)	Height of fall, H (m)			
		0.25		0.50	
		λ_{max} (m)	λ_{min} (m)	λ_{max} (m)	λ_{min} (m)
1	25.40	1.4624	0.1024	1.5846	0.1207
2	38.10	1.6389	0.1211	1.7082	0.1215
3	50.80	1.7173	0.1291	1.7297	0.1295
4	76.20	2.0148	0.1300	2.0811	0.1306

0.15 m, and in Table 3 for a receiver distance of 0.30 m. Regardless of the receiver distance, either 0.15 or 0.30 m, height of fall of the dropping mass does not result in any significant change in the values of λ_{min} and λ_{max}. Tables 2 and 3 support this fact.

The source offset concept states that the first source is equal to the receiver distance; therefore, a longer receiver distance means that the source is located further away from the receiver. Rayleigh surface waves spread cylindrically from a point source and tend to dominate the measured wave field at large distance. In simpler terms, large receiver distance allows wavelength to penetrate deeper and therefore provide information of the subsurface in the lower frequency region. This study could serve as a guide in determining the proper configuration for obtaining data within the depth of interest of the pavement layer.

The differences in λ_{min} and λ_{max} with different input source energies are plotted exclusively for receiver distance 0.15 m and are shown in Figure 6 while Figure 7 shows the plot for receiver distance of 0.30 m. It can be seen that λ_{max} increases linearly with an increase in the magnitude of input energy. This is true for both receiver distances. Figures 6 and 7 also show that λ_{min} increases with an increase in the magnitude of input energy. In other words, contrary to the maximum
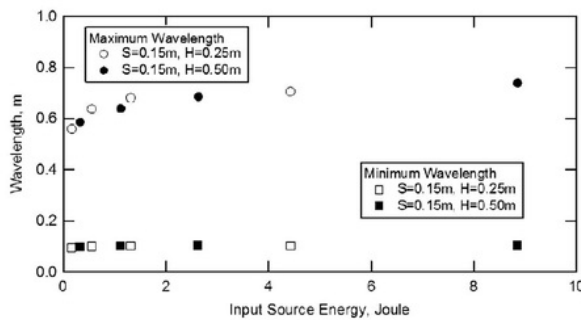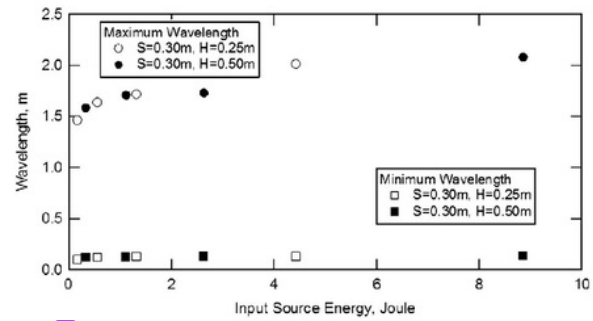

Figure 6. The effect of changes in input energy on maximum wavelength (λ_{max}) and minimum wavelength (λ_{min}) for receiver distance, $S = 0.15$ m.

Figure 7. The effect of changes in input energy on maximum wavelength (λ_{max}) and minimum wavelength (λ_{min}) for receiver distance, $S = 0.30$ m.

wavelength, the height of dropping mass and the mass of the steel ball do not have significant effect in the value of minimum wavelength.

Inversion analysis was also done to obtain the layer properties of the pavement. The shear wave velocity profiles of four cases were generated and are shown in Figure 8. SASW method uses the 'superposed' mode, which does not fall into specific normal modes (fundamental and higher modes). This is an important feature since for irregular pavement layering systems, these superposed/apparent phase velocities fall in between the normal modes. And since source location for pavement testing is also close to the receiver location, mode separation of surface wave is not practical (Stokoe *et al.* 2004). Therefore, for pavement testing, the SASW method, which incorporates superposed mode of higher mode surface waves and body waves, has a significant advantage over methods such as MASW and ReMi in terms of the application of modes for inversion analysis. The phase unwrapping procedure is also cumbersome in irregular pavement layering systems, but can be improved through signal processing technique called the Impulse Response Filtration (Stokoe *et al.* 2004).

3.2. Numerical integration of acceleration data to obtain displacement

Acceleration data are obtained from raw output voltage which is measured through acceleration sensitivity. Bandpass filtering was applied to acceleration data which was then integrated to obtain velocity. Filtration was done to remove high frequency noise and low frequency drift of the signals. Displacement was then obtained through analysis which is equivalent to integrating velocity signals after performing the filtration process. Figure 9 shows the acceleration time history obtained from Accelerometer 1 and its velocity after the first integration. The extracted data were from the measurement obtained from using Ball 4 as a source (refer to Figure 1). In the SASW method, the sensor/receiver located nearest to the source (where the load is applied) is called Accelerometer 1, while the second sensor/receiver located after the first one is named Accelerometer 2.

This makes sense since as the travelling time of the signal increases, more energy is dissipated and therefore the signal gets weaker as it reached the second sensor. This explains the higher
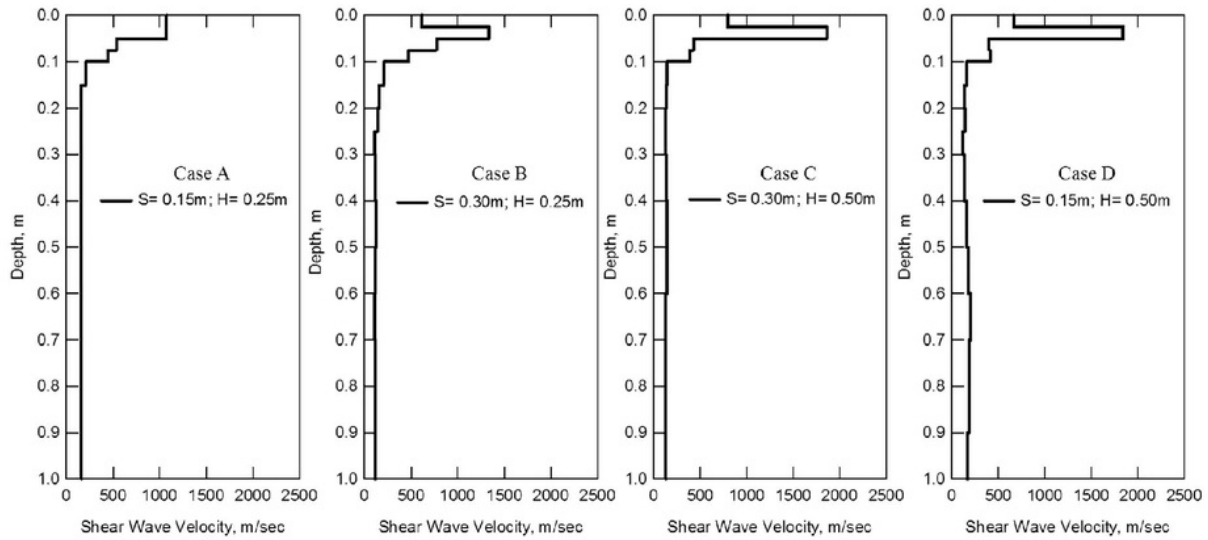
Figure 8. Shear wave velocity profiles generated for four cases: (1) Case A – receiver spacing, $S = 0.15$ m; height of falling weight, $H = 0.50$ m, (2) Case B – receiver spacing, $S = 0.15$ m; height of falling weight, $H = 0.25$ m, (3) Case C – receiver spacing, $S = 0.30$ m; height of falling weight, $H = 0.50$ m and (4) Case D – receiver spacing, $S = 0.30$ m; height of falling weight, $H = 0.25$ m.
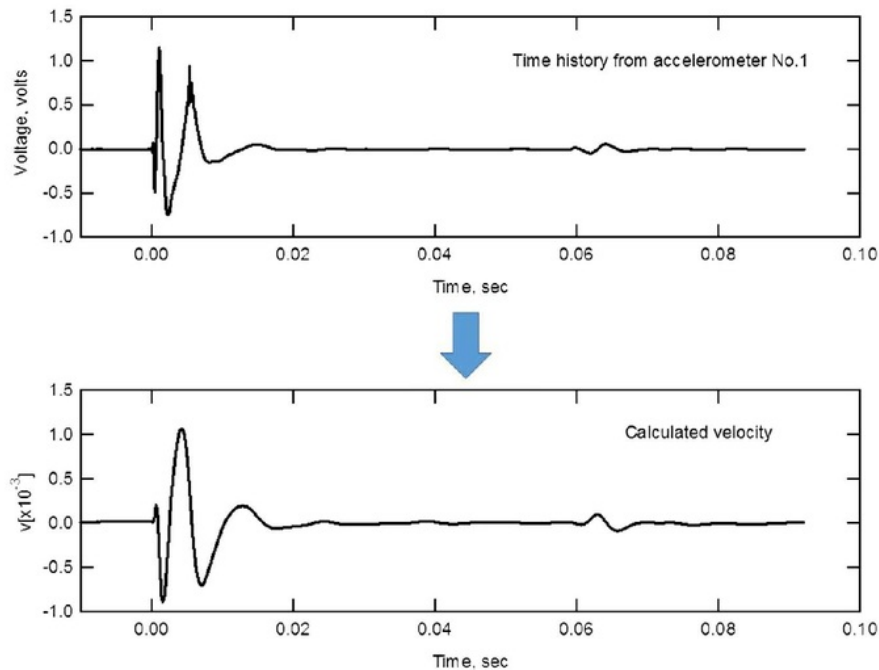

Figure 9. Calculated velocity obtained from acceleration time history recorded by accelerometer No 1.

amplitude of the signal recorded by Accelerometer 1 compared to the signal recorded by Accelerometer 2, as shown in Figure 10. Figures 9 and 10 show the velocity obtained from the first numerical integration of the acceleration signal. In this measurement record, the sampling rate is taken as 19 sample/s. The frequency span of the recorded data is 20 kHz. The time length recorded is 0.051175 s with 1024 frequency lines.

Displacement was then obtained by analysing and synthesising velocity data using Equations (2)–(5). The displacement obtained from the numerical double integration is shown in Figure 13 together with the displacement obtained through FEM. The figure will be discussed in the following section. The numerical integration produced good result, which is congruent with the displacement from FEM.
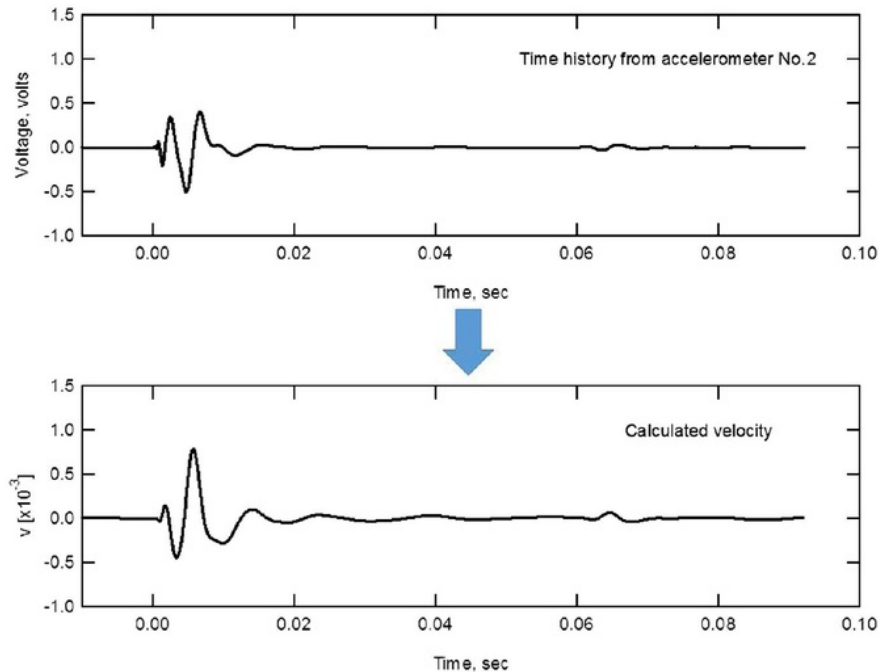
Figure 10. Calculated velocity obtained from acceleration time history recorded by accelerometer No 2.

3.3. Validation of displacement through finite element analysis

A model of layered pavement was built using commercial finite element analysis software called ABAQUS; it consists of a 0.10 m asphalt layer with a density of 2300 kg/m³, a 0.50 m base layer with a density of 2100 kg/m³ and a 0.25 m sub-base layer with a density of 2100 kg/m³. The elastic moduli of the layers are 2500, 1000 and 500 MPa, respectively. The Poisson's ratio for asphalt layer is 0.35 while the base and sub-base layers share the same Poisson's ratio of 0.4. These parameters are in accordance with the specification set by The Department of Development Management and the Public Works Department (JKR 2008). The segment of the pavement layer and its characteristics are shown in Figure 11.

An impulse force of 17.7 N was applied to the pavement layer to obtain a structural response in terms of displacement. The change in momentum occurred at 0.017 s of period in time (during the impact), and assuming that there is no energy lost, the dropped mass is calculated to be 1.805 kg, which is the mass of Ball 4 (refer to Figure 1). Damping was neglected since very little energy was dissipated over a short period of time. The analysis was performed for a period of 0.105 s with a time increment of 1×10^{-7} second.

There are many factors contributing to the dynamic deformations of road, although according to Arraigada and Partl (Arraigada and Partl 2006), it is usually likely to find very small deformations at low frequencies. This happened because very little acceleration was recorded in the low frequency region. Figure 12 shows a sequence of pictures arranged to show the
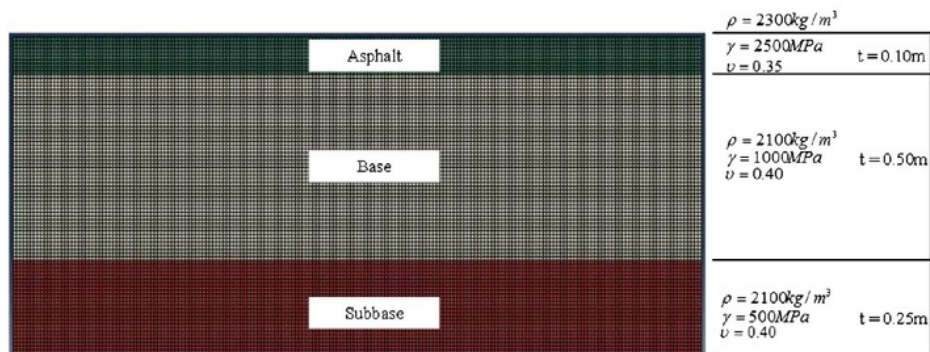

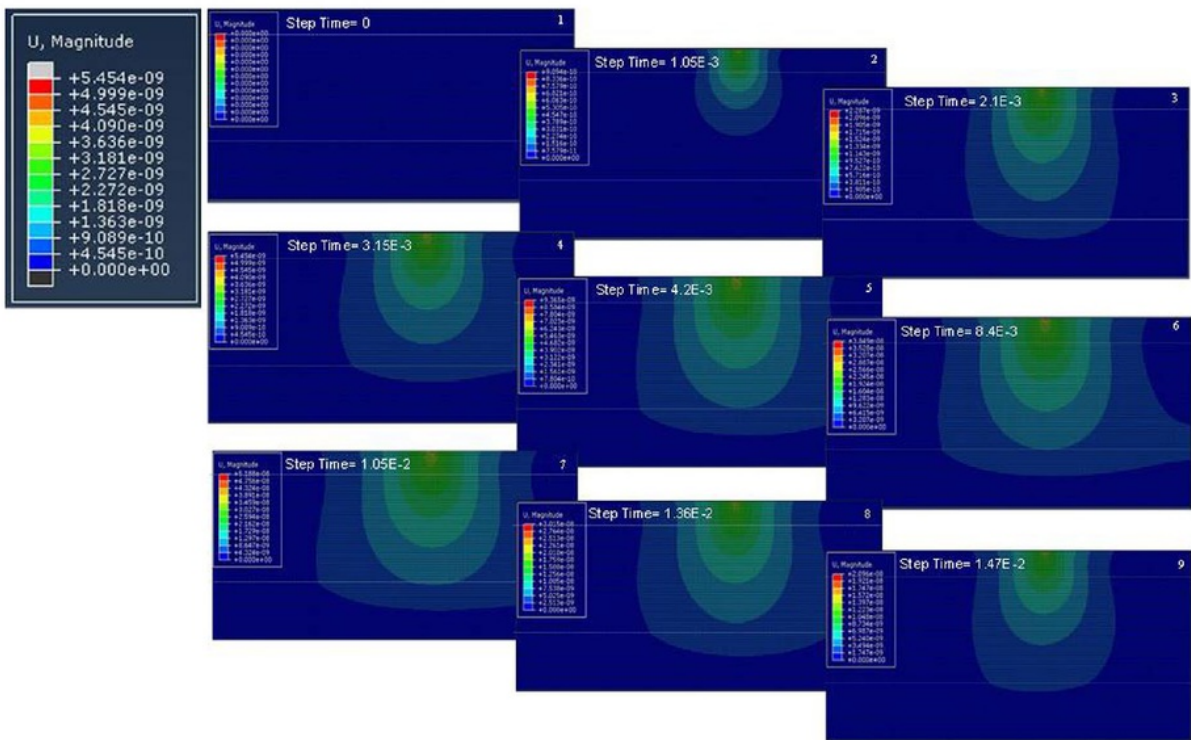**Figure 11.** The model of pavement layer built in Finite Element Analysis' software.

Figure 12. Picture in sequences from 1 to 9: deformation occurrence at the pavement layer model.
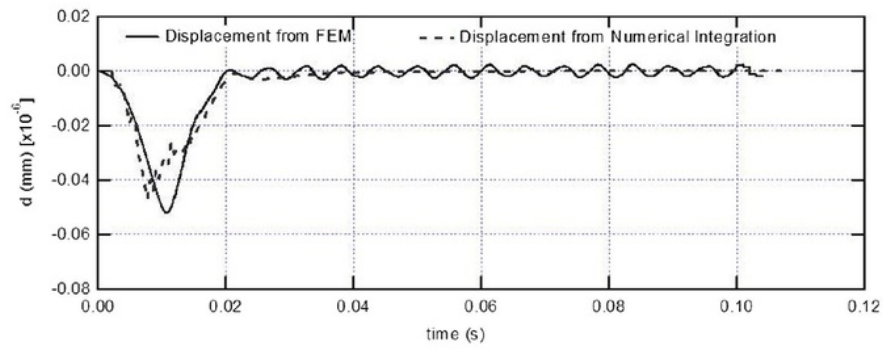
Figure 13. Comparison of displacement result obtained from numerical double integration and finite element analysis method.

occurrence of deformation in step motion during the period when the impulse force was applied to the model. Although the energy dissipates, the observed displacement was significantly small because the load applied was very small too.

The data collected post-analysis from the FEA software were plotted together with the displacement result obtained through velocity integration, and are shown in Figure 13. One apparent observation is that the displacement due to FEM resulted in lower valley compared to displacement due to numerical integration. This means that it has higher deflection. Other than that, the displacement result seems more stable during the impulse compared to the displacement obtained from numerical integration.

Peak difference could also occur because the integration procedure was adversely affected by the baseline offsets of the sensors. However, as can be seen in the figure, the later signal is smoothed out when the numerical integration method was used compared to the FEM analysis. Although it is not very significant, this could be one of the advantages of the double integration procedure.

4. Conclusion

Based on SASW test done on asphaltic pavement, the effect of input source energy on the maximum wavelength (λ_{max}) and minimum wavelength (λ_{min}) was explored. The λ_{max} increases linearly with an increase in the input source energy due to the change in the height and the mass of the dropping ball; both these factors have a significant effect on the value of λ_{max}. It can

also be concluded that both the height and mass of the dropping ball have marginal effect on the value of λ_m as the result shows that its value is almost constant even when the magnitude of the input source energy was increased.

As stated in the earlier section of this paper, measurement of road deflection due to traffic loading could be done in a simple manner through the use of accelerometers. This, with the help of POLLCA, could provide many advantages, especially in terms of handling and mobility. It could be a low-cost solution for the measurement of road deflection in industry. The validity of using accelerometers as sensors to measure displacement was also verified using the finite element analysis software which gives good results when comparison was made. This study can be used as a guide for determining the receiver and array configuration in an SASW test on any pavement site. Researchers could also use accelerometers as sensors to evaluate road deflection.

Acknowledgement

Disclosure statement

No potential conflict of interest was reported by the authors.

Funding

ORCID

Amiruddin Ismail ⓘ http://orcid.org/0000-0001-6547-8169

References

Arraigada, M. and Partl, M., 2006. Calculation of displacements of measured accelerations, analysis of two accelerometers and application in road engineering. *In: 6th Swiss transport research conference*, 15–17 March, Monte Verita/Ascona.

Barness, C.L. and Trottier, J.F., 2009a. Evaluating high-frequency viscoelastic moduli in asphalt concrete. *Research in Nondestructive Evaluation*, 20 (2), 116–130.

Barness, C.L. and Trottier, J.F., 2009b. Hybrid analysis of surface wave field data from Portland cement and asphalt concrete plates. *NDT & E International*, 42 (2), 106–112.

Bowness, D., *et al.*, 2007. Monitoring the dynamic displacements of railway track. *Proceedings of the Institution of Mechanical Engineers, Part F: Journal of Rail and Rapid Transit*, 221 (1), 13–22.

Gucunski, N. and Woods, R.D., 1991. Instrumentation for SASW Testing. *In: Geotechnical Special Publication No 29. Recent Advances in Instrumentation, Data Acquisition and Testing in Soil Dynamics*. American Society of Civil Engineers, 1–16.

Gucunski, N. and Woods, R.D., 1992. Numerical simulation of the SASW test. *Soil Dynamics and Earthquake Engineering*, 11, 213–227.

Hall, L., 2003. Simulations and analyses of train-induced ground vibrations in finite element models. *Soil Dynamics and Earthquake Engineering*, 23, 403–413.

Heisey, J.S., Stokoe, K.H. II, and Meyer, A.H., 1982. Moduli of pavement systems from spectral analysis of surface waves. *Transportation Research Record*, 852, 22–31.

Jiang, H., *et al.*, 2016. Simulating train moving loads in physical model testing of railway infrastructure and its numerical calibration. *Acta Geotechnica*, 11 (2), 231–242.

Jiang, H., *et al.*, 2016. Dynamic performance of high-speed railway formation with the rise of water table. *Engineering Geology*, 206, 18–32.

Joh, S.-H., Rosenblad, B. L., and Stokoe II, K.H., 1997. Improved data interpretation method for SASW Tests at complex geotechnical sites. *International Society of Offshore and Polar Engineering*, 1, 875–881.

Joh, S.H., *et al.*, 2014. Alleviation of numerical instability in geophone-based measurement of track vibrations by utilizing a priori information. *KSCE Journal of Civil Engineering*, 18 (5), 1351–1358.

Jones, R., 1962. Surface wave technique for measuring the elastic properties and thickness of roads: theoretical development. *British Journal of Applied Physics*, 13 (1), 21–29.

Kausel, E. and Roesset, J.M., 1981. Stiffness matrices for layered soils. *Bulletin of the Seismological Society of America*, 71 (6), 1743–1761.

Kumar, J., 2011. A study on determining the theoretical dispersion curve for Rayleigh wave propagation. *Soil Dynamics and Earthquake Engineering*, 31 (8), 1196–1202.

Kumar, J. and Hazra, S., 2014a. SASW testing of asphaltic pavement by dropping steel balls. *International Journal of Geotechnical Engineering*, 8 (1), 34–45.

Kumar, J. and Hazra, S., 2014b. Effect of input source energy on SASW evaluation of cement concrete pavement. *Journal of Materials in Civil Engineering*, 26 (6), 1–7.

Kumar, J. and Naskar, T., 2015. Effects of site stiffness and source to receiver distance on surface wave tests' results. *Soil Dynamics and Earthquake Engineering Journal*, 77 (1), 71–82.

Kumar, J. and Rakaraddi, P.G., 2012. On the height of fall of dropping mass in SASW measurements for asphaltic road pavements. *International Journal of Pavement Engineering*, 13 (6), 485–493.

Kumar, J. and Rakaraddi, P.G., 2013a. SASW evaluation of asphaltic and cement concrete pavements using different heights of fall for a spherical mass. *International Journal of Pavement Engineering.*, 14 (4), 354–363.

Kumar, J. and Rakaraddi, P.G., 2013b. Effect of source energy for SASW testing on geological sites. *Geotechnical and Geological Engineering*, 31 (1), 47–66.

Lin, C.P. and Lin, C.H., 2007. Effect of lateral heterogeneity on surface wave testing: numerical simulations and a countermeasure. *Soil Dynamics and Earthquake Engineering*, 27, 541–552.

Nazarian, S., 1984. *In situ determination of elastic moduli of soil deposits and pavement systems by spectral analysis of surface waves method*. Dissertation (PhD). The University of Texas.

Nazarian, S. and Desai, M. R., 1993. Automated surface wave method: field testing. *Journal of Geotechnical Engineering*, 119 (7), 1094–1111. American Society of Civil Engineers.

Nazarian, S. and Stokoe II, K. H., 1986. *In-situ determination of elastic moduli of pavement systems by spectral analysis of surface waves method (theoretical aspects)*. Austin: Centre for Transportation Research, University of Texas, Research Report 437-2.

Nazarian, S. Stokoe II, *et al.*, 1988. Determination of pavement layer thickness and moduli by SASW method. *Transportation Research Record*, 1196, 133–150.

Priest, J.A. and Powrie, W., 2009. Determination of dynamic track modulus from measurement of track velocity during train passage. *Journal of Geotechnical and Geoenvironmental Engineering*, 135, 1732–1740.

Rix, G. and Stokoe, K.H. II, 1989. Stiffness profiling of pavement subgrades. *Transportation Research Record*, 1235, 1–9.

Roberts, G. W., Meng, X., and Dodson, A.H., 2001. The use of kinematic GPS and Triaxial accelerometers to monitor the deflections of large bridges. *In: International Federation of Surveyors (FIG) and Working Group 6.1 eds. Deformation measurements and analysis, 10th International symposium on deformation measurements*, 19–22 March. Orange, CA, 268–275.

Roesset, J.M., 1998. Nondestructive dynamic testing of soils and pavements. *Tamkang Journal of Science and Engineering*, 1 (2), 61–81.

Roesset, J. M., *et al.*, 2011. Impact of weight falling onto the ground. *Journal of Geotechnical Engineering*, 120 (8), 1394–1412. American Society of Civil Engineers.

Sayeed, M.A. and Shaheen, M.A., 2016. Three-dimensional numerical modelling of ballasted railway track foundations for high-speed trains with special reference to critical speed. *Transportation Geotechnics*, 6, 55–65.

Simonin, J., *et al.*, 2009. Deflection measurement: the need of a continuous and full view approach. *In*: E. Tutumluer and I.L. Al-Qadi, eds. *Bearing capacity of roads, railways and airfields*. London: Taylor & Francis Group, 467–476.

Stokoe II, K., *et al.*, 1994. Characterization of geotechnical sites by SASW method. *In*: R.D. Woods, ed. Technical review: geotechnical characterization of sites ISSMFE technical committee 10. New Delhi: Oxford.

Stokoe II, K.H., Joh, S.H, and Woods, R.D., 2004. Some contributions of in situ geophysical measurements to solving geotechnical engineering problems. *In*: A. Viana da Fonseca and P.W. Mayne, eds. *Proceedings ISC-2 on geotechnical and geophysical site characterization*. Rotterdam: Millpress, 97–132.

IJPE_Effect of input_Q1_2019

Materials and Pavement Design, 2007.
Publication

6   Lin, Y.-C., S.-H. Joh, and K. H. Stokoe. "Analyst J: Analysis of the UTexas 1 Surface Wave Dataset Using the SASW Methodology", Geo-Congress 2014 Technical Papers, 2014.
Publication

1%

7   Jyant Kumar. "On the height of fall of dropping mass in SASW measurements for asphaltic road pavements", International Journal of Pavement Engineering, 2011
Publication

1%

8   Jan Dirk Biesheuvel, Jeroen J. Briaire, Monique A. M. de Jong, Stefan Boehringer, Johan H. M. Frijns. "Channel discrimination along all contacts of the cochlear implant electrode array and its relation to speech perception", International Journal of Audiology, 2019
Publication

<1%

9   Jianliang Qian, Yong-Tao Zhang, Hong-Kai Zhao. "A Fast Sweeping Method for Static Convex Hamilton–Jacobi Equations", Journal of Scientific Computing, 2007
Publication

<1%

10 Insan Arafat Jamil, Minhaz Ibna Abedin, Dhiman Kumar Sarker, Jahedul Islam. "Vibration data acquisition and visualization

<1%

system using MEMS accelerometer", 2014 International Conference on Electrical Engineering and Information & Communication Technology, 2014

Publication

---

11   Lin, Chih-Ping, Chun-Hung Lin, Yung-Zheng Dai, and Chih-Jung Chien. "Assessment of Ground Improvement with Improved Columns by Surface Wave Testing", Grouting and Deep Mixing 2012, 2012.   <1%

Publication

---

12   Ivan Isailović, Michael P. Wistuba, Augusto Cannone Falchetto. "Investigation on mixture recovery properties in fatigue tests", Road Materials and Pavement Design, 2017   <1%

Publication

---

13   Zywicki, Daren J., and Glenn J. Rix. "Mitigation of Near-Field Effects for Seismic Surface Wave Velocity Estimation with Cylindrical Beamformers", Journal of Geotechnical and Geoenvironmental Engineering, 2005.   <1%

Publication

---

14   Hailiang Sun, Yanyang Zi, Zhengjia He, Jing Yuan, Xiaodong Wang, Lue Chen. "Customized Multiwavelets for Planetary Gearbox Fault Detection Based on Vibration Sensor Signals", Sensors, 2013   <1%

Publication

15 Chih-Ping Lin, Chun-Hung Lin. "Effect of lateral heterogeneity on surface wave testing: Numerical simulations and a countermeasure", Soil Dynamics and Earthquake Engineering, 2007
Publication

<1%

16 Sayantan Chakraborty, Tejo V. Bheemasetti, Anand J. Puppala, Louie Verreault. "Use of Constant Energy Source in SASW Test and Its Influence on Seismic Response Analysis", Geotechnical Testing Journal, 2019
Publication

<1%

17 Haidar Samet, Sara Gashtasbi, Nima Tashakor, Teymoor Ghanbari. "Improvement of reactive power calculation in electric arc furnaces utilising Kalman filter", IET Science, Measurement & Technology, 2017
Publication

<1%

18 "Environmental Vibrations and Transportation Geodynamics", Springer Nature, 2018
Publication

<1%

19 Joh, Sung-Ho, Kenneth H. Stokoe, II, Il-Wha Lee, Tae-Ho Kang, Brent Rosenbld, and James A. Bay. "Joint Inversion for Apparent Phase Velocities of Rayleigh and Love Waves", GeoCongress 2006, 2006.
Publication

<1%

20   Shyh-Chyang Lin. "Monitoring of concrete building construction", Canadian Journal of Civil Engineering, 10/2007
Publication

<1%

21   B Coelho. "An assessment of transition zone performance", Proceedings of the Institution of Mechanical Engineers Part F Journal of Rail and Rapid Transit, 01/01/2010
Publication

<1%

22   "Geotechnical Characterisation and Geoenvironmental Engineering", Springer Nature, 2019
Publication

<1%

23   Roesset, Jose M., Eduardo Kausel, Vicente Cuellar, Jose L. Monte, and Julian Valerio. "Impact of Weight Falling onto the Ground", Journal of Geotechnical Engineering, 1994.
Publication

<1%

24   N. Gucunski, R.D. Woods. "Numerical simulation of the SASW test", Soil Dynamics and Earthquake Engineering, 1992
Publication

<1%

Exclude quotes	On	Exclude matches	< 10 words
Exclude bibliography	On		